ISSN (Print) 1226-1750
ISSN (Online) 2233-6656
Journal of Magnetics 28(4), 409-414 (2023) https://doi.org/10.4283/JMAG.2023.28.4.409

Development of PET Detector for Localization Using MLPE Based on Simulation Data

Seung-Jae Lee[1,2]*, Byungdu Jo[1,2], and Sun-Young Cho[3]

[1]*Department of Radiological Science, Dongseo University, Busan 47011, Republic of Korea*
[2]*Center for Radiological Environment & Health Science, Dongseo University, Busan 47011, Republic of Korea*
[3]*Department of Occupational Therapy, Sangji University, Won-Ju 26399, Republic of Korea*

(Received 22 September 2023, Received in final form 29 November 2023, Accepted 5 December 2023)

In order to measure the position of the scintillation pixel of the positron emission tomography (PET) detector module, it is necessary to obtain a flood image through a radiation source and then perform a segmentation process of each scintillation pixel area in the flood image. Without performing this process, a method of reading the scintillation pixel position using simulation data was developed. It was difficult to directly apply the data obtained through simulation to the experimental data since simulation data and experimental data cannot be directly matched. In this study, the Anger data of four channels obtained from the detector module composed of simulation were calculated at the ratio according to the channel and applied to the experimental data. Through simulation, a look-up table (LUT) for each scintillation pixel was prepared, and the position of the scintillation pixel where the gamma ray event occurred was measured using the experimental data and the maximum likelihood position estimation (MLPE). The measurement result showed an accuracy of 94.4 %. If these study results are introduced into the PET detector module, the position of the scintillation pixel can be read quickly and conveniently without changing the existing system.

Keywords : positron emission tomography (PET), Simulation data, maximum likelihood position estimation (MLPE), DETECT2000, electromagnetic radiation, magnetic field

1. Introduction

Positron emission tomography (PET) measures an interaction position between gamma rays generated by an annihilation of positrons and scintillation pixels of a detector to obtain molecular imaging. At this time, the image is reconstructed by connecting a line of response (LOR) with the scintillation pixel of the detector measured simultaneously in the 180-degree direction [1, 2]. In order to measure the position of the scintillation pixel interacting with gamma rays, a flood image of the scintillation pixel of the detector is first obtained, and then the imaged area of each scintillation pixel is segmented. The position of the scintillation pixel of the detector is subsequently specified through the position of the image region reconstructed based on the signal generated by the new gamma ray incident. All processes are carried out through experimental data acquisition. In this study, a method was developed to characterize the position of scintillation pixels interacting with gamma rays by using simulation data without performing a series of processes for acquiring a flood image and segmenting regions. Applying simulation data directly to experiments pose many difficulties. This is because the simulation data and experimental data do not match on a 1:1 ratio. To solve this problem, the ratio of each acquired data was used. The ratio of data acquired through simulation and the ratio of data acquired through the experiment can be directly compared. The detector was designed using the DETECT2000 [3, 4] simulation tool, which can simulate the behavior of light in a scintillator. The ratio of signals in all the scintillation pixels of the detector was prepared as a lookup table (LUT). The position of the scintillation pixel was characterized using the data obtained from the experiment and the maximum likelihood position estimation (MLPE) [5, 6].

*Corresponding author: Tel:
Fax: , e-mail: sjlee@gdsu.dongseo.ac.kr

2. Material and Methods

2.1. Detector design for DETECT2000 simulation

The detector was designed as shown in Fig. 1 using the DETECT2000 simulation tool to create LUT through simulation. The entire detector was designed by arranging 2 mm × 2 mm × 10 mm scintillation pixels in a 6 × 6 array and a photosensor with 3 mm × 3 mm pixels in a 4 × 4 array to collect light generated in the scintillation pixel. The pitch between scintillation pixels is 2.1 mm, the overall size is 12.5 mm × 12.5 mm × 10 mm, and the photosensor is arranged with a 3.2 mm pitch, so the overall size is 12.6 mm × 12.6 mm. In order to move the light generated by the interaction between the scintillation pixel and the gamma ray to the photosensor, all surfaces of the scintillation pixel except for the side coupled to the photosensor were treated as reflectors. An optical grease [7] was used between the scintillation pixel and the photosensor to minimize light loss due to rapid refractive index changes. The scintillation pixel used in the detector design is GAGG [8-10], which has a density of 6.7 g/cm^3, suitable for detecting high-energy gamma rays, and a light generation amount of ~54,000 photons/MeV, which generates a considerable amount of light and has excellent energy resolution characteristics. For the photosensor, the detector was designed using SensL's Matrix9 [11] system, which is composed with a silicon photomultiplier (SiPM) array. This photosensor has the highest quantum efficiency of 41 % at a light wavelength of 420 nm as well as excellent quantum efficiency in a wide range of light wavelengths. It has excellent quantum efficiency of about 25 % in the light wavelength range generated by the GAGG scintillator.

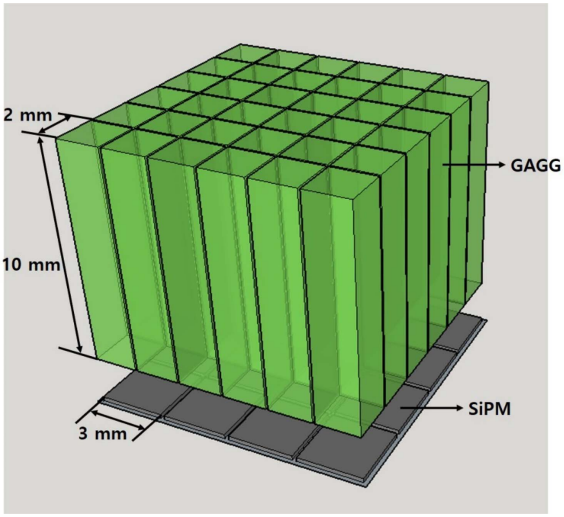

Fig. 1. (Color online) Detector designed using the DETECT2000 simulation tool. The GAGG scintillation pixels of 2 mm × 2 mm × 10 mm were configured in a 6 × 6 array, and the photosensor was composed of 3 mm × 3 mm SiPM in a 4 × 4 array to design the entire detector.

2.2. LUT creation

In the detector designed in this study, light was generated at the center of all scintillation pixels as shown in Fig. 2 to create LUT for gamma-ray events generated from each scintillation pixel. In Fig. 2, the red arrow indicates an example of the light path generated by the gamma ray event. For the number of generated lights, the light generation amount of the GAGG scintillator and the quantum efficiency of the SiPM were applied to the annihilation radiation energy as shown in the following equation.

$$\text{Light Photons} = \text{Radiation Energy} \times \text{GAGG light yield} \times \text{SiPM PDE} \quad (1)$$

The light generated from the center of each scintillation pixel is finally acquired by the SiPM after going through

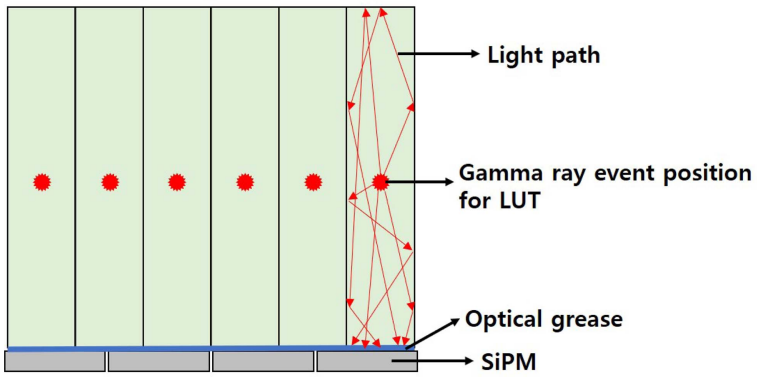

Fig. 2. (Color online) A schematic diagram of the path of light generated by the gamma ray event coming from the center of all scintillation pixels. Red arrows indicate examples of light path.

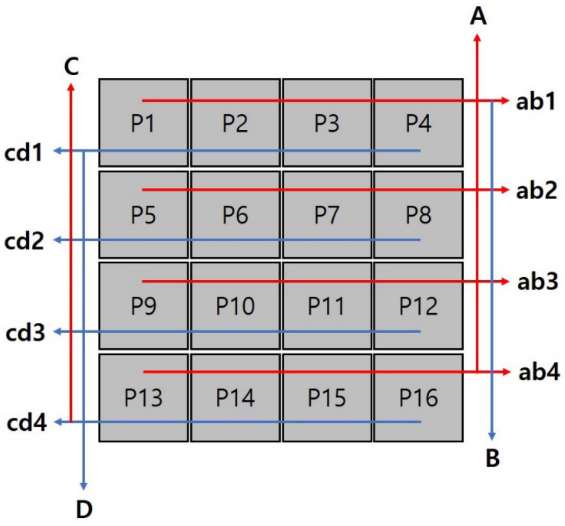

Fig. 3. (Color online) A schematic diagram of summing and reducing 16 channel signals into 4 channel signals. The reduction to 4 channels was done by adding weights according to the distance where the SiPM pixels are located.

processes such as movement, reflection, and scattering in the scintillator. The light signals obtained from the 16 channels of the SiPM were summed and reduced to 4 channels, A, B, C, and D, as shown in Fig. 3. Each channel was summed according to the following equation by giving a weight according to the distance of the SiPM pixel [12].

$$\begin{aligned} ab1 &= (w_1 \times P1) + (w_2 \times P2) + (w_3 \times P3) + (w_1 \times P4) \\ ab2 &= (w_1 \times P5) + (w_2 \times P6) + (w_3 \times P7) + (w_1 \times P8) \\ ab3 &= (w_1 \times P9) + (w_2 \times P10) + (w_3 \times P11) + (w_1 \times P12) \\ ab4 &= (w_1 \times P13) + (w_2 \times P14) + (w_3 \times P15) + (w_1 \times P16) \\ cd1 &= (w_4 \times P1) + (w_3 \times P2) + (w_2 \times P3) + (w_1 \times P4) \\ cd2 &= (w_4 \times P5) + (w_3 \times P6) + (w_2 \times P7) + (w_1 \times P8) \\ cd3 &= (w_4 \times P9) + (w_3 \times P10) + (w_2 \times P11) + (w_1 \times P12) \\ cd4 &= (w_4 \times P13) + (w_3 \times P14) + (w_2 \times P15) + (w_1 \times P16) \end{aligned} \quad (2)$$

Here, $P1$, $P2$,, …, $P16$ indicate signals obtained from SiPM pixels, while ab1, ab2, ab3, ab4, cd1, cd2, cd3, and cd4 indicate signals summed by giving weights (w_i) according to the distances for each SiPM line. Finally, as shown in the following equation, A is calculated as the sum of signals weighted according to the distances of ab1, ab2, ab3, and ab4. The signals of B, C, and D are similarly calculated as the sum of the weighted signal.

$$\begin{aligned} A &= (w_4 \times ab1) + (w_3 \times ab2) + (w_2 \times ab3) + (w_1 \times ab4) \\ B &= (w_1 \times ab1) + (w_2 \times ab2) + (w_3 \times ab3) + (w_4 \times ab4) \\ C &= (w_4 \times ab1) + (w_3 \times ab2) + (w_2 \times ab3) + (w_1 \times ab4) \\ D &= (w_4 \times ab1) + (w_2 \times ab2) + (w_3 \times ab3) + (w_4 \times ab4) \end{aligned} \quad (3)$$

The signal for each channel was acquired through 1,000 gamma ray events for each position, and the signal reduced by summing to 4 channels was divided into channel A while the LUT was created as a ratio for channel A. That is, LUT was created by calculating the average value and standard deviation value by A/A, B/A, C/A, and D/A.

2.3. Experimental data acquisition

In order to apply the LUT created through simulation to the experimental data, experimental settings for data acquisition were established as shown in Fig. 4. A scintillator consisting of GAGG scintillation pixels in a 6

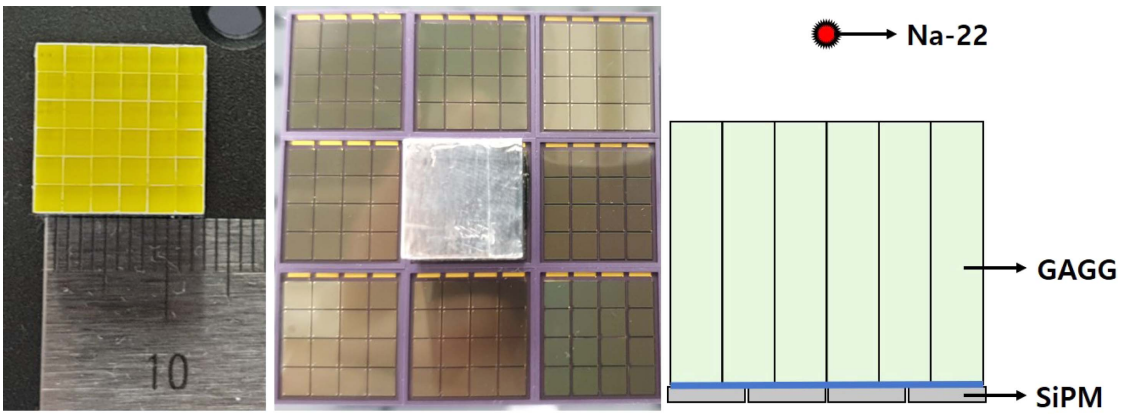

Fig. 4. Experimental settings for applying LUTs created using simulation data to data obtained through experiments. The image on the left shows a GAGG scintillator in a 6 × 6 array, the middle image shows a GAGG scintillator combined with SiPM, and the image on the right shows a schematic diagram for acquiring data using a Na-22 radiation source.

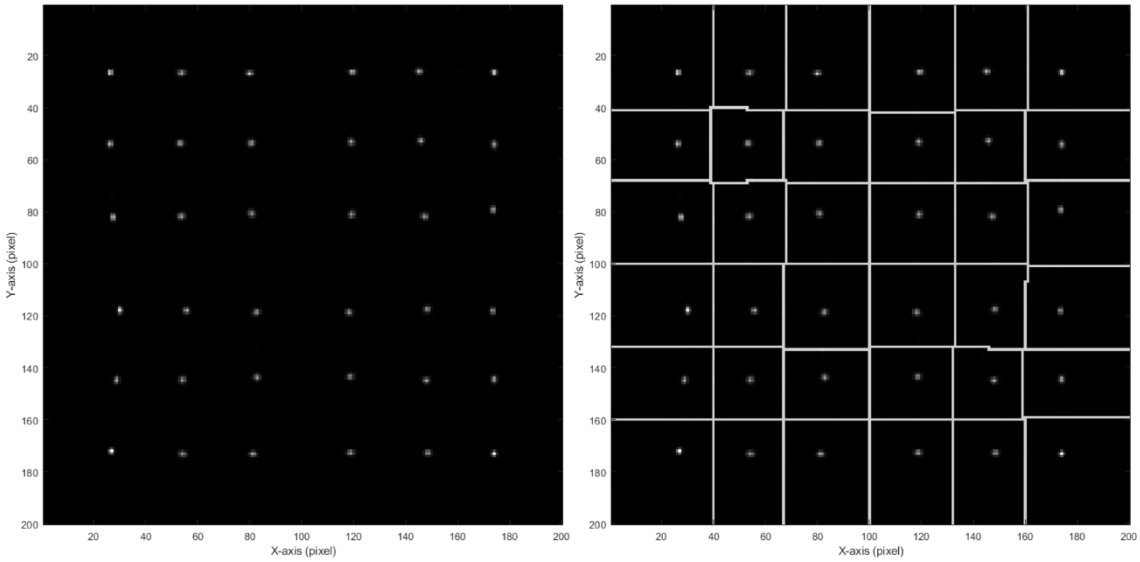

Fig. 5. Flood image reconstructed using data acquired through SiPM of the light generated by the interaction of the GAGG scintillator and gamma rays, and a pixel segmented image.

× 6 array and a SiPM consisting of a 4 × 4 pixel array were used to construct the detector. Using a Na-22 radiation source that generates annihilation radiation, light generated from GAGG was acquired from a 16-channel SiPM. The signals obtained from each SiPM pixel were reduced to four channels A, B, C, and D by summing after applying a weight according to distance. The flood image was reconstructed using 4 channels, and signals for 6 × 6 scintillation pixels were individually separated through pixel segmentation. The separated signals were processed by calculating the ratio for the A channel in the same way as the LUT that was created by simulation.

2.4. Positioning using MLPE

The MLPE is a function that calculates the input value closest to the mean value using the mean and standard deviation. Through the mean value and standard deviation value of the prepared LUT, the position of the scintillation pixel can be determined by comparing it with the experimental data. The MLPE equation is followings

$$\ln \Pr[M_i|x] = -\left(\Sigma_{i=1}^{n} \frac{(M_i - \mu(x))^2}{2\sigma_i^2(x)} + \Sigma_{i=1}^{n} \ln \sigma_i(x) \right) \quad (4)$$

Here, M is the ratio of the experimental data signals for 4 channels, μ is the mean value in the LUT, and σ is the standard deviation value. Since it is expressed as a ratio for channel A which is always 1 except for this, the ratio of the three channels is actually entered to the MLPE to determine the position.

3. Results and Discussion

Using the LUT created through simulation and the ratio of 4 channel signals of each scintillation pixel obtained through the experiment, the scintillation pixel positioning

Table 1. Positioning accuracy of a GAGG pixel measured using simulated LUT and MLPE for the experimental data of each GAGG pixel. [unit: %]

Accuracy	X1	X2	X3	X4	X5	X6
Y1	99.1	97.1	96.1	95.4	96.6	93.3
Y2	93.6	96.5	96.4	95.3	97.9	96.1
Y3	90.5	94.0	90.6	91.5	95.2	91.5
Y4	90.9	98.2	94.7	91.5	96.1	91.9
Y5	93.7	96.0	94.1	95.6	97.3	92.5
Y6	93.9	96.1	93.9	91.9	93.1	91.5

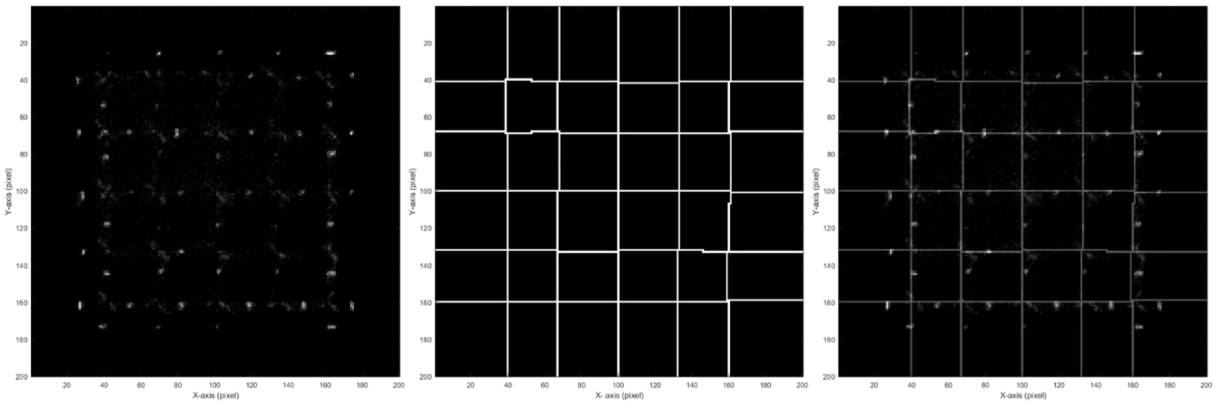

Fig. 6. Error image for positioning of scintillation pixels measured from experimental data using simulated LUT. Left: error image, middle: segmentation map, right: combined image.

accuracy was measured through the MLPE. Signals for each scintillation pixel were individually classified through pixel segmentation after obtaining a flood image. Accuracy was measured through comparative analysis with the LUT of the simulation using these separated signals. Fig. 5 represents a flood image and regions segmented for each scintillation pixel. It can be seen that the regions of all scintillation pixels are clearly separated. Table 1 shows the positioning accuracy results of the scintillation pixels calculated through the MLPE for each scintillation pixel. Excellent results were obtained with an average accuracy of 94.4 ± 2.3 % in all positions. The highest accuracy was 99.1 % at the scintillation pixel coordinates (1, 1) and the lowest accuracy was 90.5 % at (1, 3). The position where the error occurred is shown in Fig. 6. It can be seen that errors occur mainly between scintillation pixels. The signal whose position is measured as an intermediate point appears as an error in the process of specifying the position of the scintillation pixel. The location accuracy of this study method was calculated by using the data on the individual images of each scintillation pixel through segmentation after acquiring the flood image. The limitation is that the data of each individual scintillation pixel cannot be clearly distinguished during the segmentation process. It is considered that if there is a clear distinction, more accurate accuracy claculations will be achieved.

4. Conclusion

In this study, the position of the scintillation pixel was specified based on the signal of the photosensor obtained through the experiment using the LUT and MLPE created through simulation. It was difficult to directly match the data obtained by simulation due to the difference with the experimental data. However, it was possible to apply simulation data to experimental data by expressing the obtained data as a ratio. The signal of each scintillation pixel acquired in the experiment was compared with the LUT by calculating the 4-channel signals acquired through the conventional Anger calculation as a ratio for one channel and using it as input data for the LUT and MLPE. Analysis made it possible to characterize the position of the scintillation pixels. If the results obtained in this study are applied to a detector that measures the position using a scintillation pixel, a system capable of specifying the position of a scintillation pixel can be constructed without changing the existing system.

Acknowledgement

This work was supported by Dongseo University, "Dongseo Cluster Project" Research Fund of 2023 (DSU-20230003).

References

[1] M. E. Phelps, E. J. Hoffman, N. A. Mullani, and M. M. Ter-Pogossian, J. Nucl. Med. **16**, 210 (1975).
[2] A. K. Shukla and U. Kumar, J. Nucl. Med. **31**, 13 (2006).
[3] F. Cayouette, C. Moisan, N. Zhang, and C. J. Thompson, IEEE Trans. Nucl. Sci. **49**, 624 (2002).
[4] F. Cayouette, N. Zhang, and C. J. Thompson, IEEE Trans. Nucl. Sci. **50**, 339 (2003).
[5] H. H. Barrett, W. C. J. Hunter, B. W. Miller, S. K. Moore, Y. Chen, and L. R. Furenlid, IEEE Trans. Nucl. Sci. **56**, 725 (2009).
[6] Y. H. Chung, S.-J. Lee, C.-H. Baek, and Y. Choi, Nucl. Instrum. Methods Phys. Res. A **593**, 588 (2008).
[7] G. Romanchek, Y. Wang, H. Marupudi, and S. Abbaszadeh, Sensors **20**, 6092 (2020).

[8] K. Kamada, T. Yanagida, T. Endo, K. Tsutumi, Y. Usuki, M. Nikl, Y. Fujimoto, A. Fukabori, and A. Yoshikawa, J. Cryst. Growth **352**, 88 (2012).
[9] K. Kamada, T. Yanagida, J. Pejchal, M. Nikl, T. Endo, K. Tsutsumi, Y. Fujimoto, A. Fukabori, and A. Yoshikawa, IEEE Trans. Nucl. Sci. **59**, 2112 (2012).
[10] M. Makek, D. Bosnar, A. M. Kozuljevic, and L. Pavelic, Crystals **10**, 1073 (2020).
[11] J. Du, J. P. Schmall, Y. Yang, K. Di, E. Roncali, G. S. Mitchell, S. Buckley, C. Jackson, and S. R. Cherry, Med. Phys. **42**, 585 (2015).
[12] M. Seo, H. Park, and J. S. Lee, Electronics **10**, 698 (2021).